14th Asia-Pacific Conference on Combustion
Kaohsiung Exhibition Center, Kaohsiung, Taiwan
14th-18th May 2023

The Impact of Soret Diffusion on the Product Gas Characteristics of Premixed Laminar Ammonia/Hydrogen/Air Flames Stabilised in a Stagnation Flow

Marina Kovaleva[1,*], Gabriel J. Gotama[2], Akihiro Hayakawa[2], Ekenechukwu C. Okafor[3], Sophie Colson[2], Andrew Crayford[1], Taku Kudo[2], Hideaki Kobayashi[2]

[1]College of Physical Sciences and Engineering, Cardiff University, Cardiff CF24 3AA, United Kingdom

[2]Institute of Fluid Science, Tohoku University, 2-1-1 Katahira, Aoba-ku, Sendai, Miyagi 980-8577, Japan

[3]Faculty of Engineering, Kyushu University, 744 Motooka, Nishi-ku, Fukuoka, 819-03965, Japan

Abstract

Accurate prediction of ammonia/hydrogen flame emissions is important towards an efficient low-carbon energy future and requires accurate modelling of molecular diffusion to account for hydrogen's high diffusivity. The present work investigates the contribution of the Soret effect to molecular diffusion in a laminar burner-stabilised stagnation flame configuration using a blend of ammonia/hydrogen/air. Addition of the Soret effect in the diffusion model changes the predicted emissions of NO, increases the prediction of NO_2, and reduces N_2O and H_2 predictions. Diffusion flux analysis shows that the Soret effect acting directly on the molecule is predominantly responsible for changes in NO_2 and H_2 profiles. However, NO and N_2O emissions were indirectly affected by Soret diffusion through a change in rates of reaction involving these molecules. In the lean condition, the Soret effect drives enrichment in the flame zone through promoting H_2 diffusion towards the flame front and shifting the flame upstream. In the rich condition, enrichment of the post-flame zone through enhanced NH_3 and H_2 diffusion increases reaction rates of NO and shifts the flame downstream. Therefore, this study informs the underlying behaviours of the Soret effect in influencing ammonia/hydrogen flame chemistry.

1 Introduction

For a low-carbon energy future that accounts for the low reactivity and slow burning rate of ammonia, binary fuel blends of ammonia/hydrogen are an effective choice. Therefore, many studies, for example the work of Otomo et al. [1] explore the emissions chemistry of these blends. Accurate chemistry modelling requires a good description of the chemical kinetics and transport models. Unfortunately, the latter has to date received far less attention, with Brown et al. [2] stating that many studies focus on quantifying the error present in kinetic reaction mechanisms, while similar efforts have not been directed towards characterizing error in molecular transport models. One aspect of transport modelling therefore needing further study is variation due to molecular diffusion modelling (MDM), which involves calculation of mass transport occurring due to a species concentration gradient (ordinary diffusion), and temperature gradient (diffusion due to the Ludwig-Soret effect), with preferential (faster) diffusion being exhibited by light molecules, such as H_2 [3]. Notable works characterising the importance of MDM include a study by Fillo et al. [4] which reported 10-20% error in ordinary diffusion flux modelling when mixture-averaged rather than multicomponent formulation was used. Interestingly, a study on turbulent DNS flames by Chi et al. [5] suggested that difference in MDM had negligible effects on the flame structure and NO emissions, though impacted NO production rate and turbulent flame speed. The study also suggested that increased turbulence intensity supresses MDM effects..

Other studies on the effect of Soret diffusion in hydrogen/air and hydrocarbon/hydrogen/air flames [6,7], show that H_2 and H molecules are the dominant contributor to Soret diffusion, explained by accelerated hydrogen diffusion towards the flame front and a higher peak temperature flame driven by a relatively richer effective mixture [8]. Netzer et al. [9] studied ammonia/hydrogen wrinkled laminar premixed flames, suggesting that the Soret effect further reinforces the preferential diffusion of hydrogen, supporting local equivalence ratio enrichment in convex shaped portions of the flame front. Although studies suggest that the Soret effect should not be overlooked for flames containing a high hydrogen pool [10,11], an understanding of the impact of the Soret effect on ammonia/hydrogen chemistry has not been fully developed.

Therefore, the present study utilises a 1D laminar stagnation flame model to understand the effects of MDM at the flame zone and post-flame zone wall quenching regions. Diffusion flux results identified the flame regions and dominant species where the Soret effect has the greatest influence on mass diffusion rate and flame properties.

2 Methodology

The present modelling configuration is detailed by the experimental work of Hayakawa et. al [12] on laminar premixed burner stagnation flames of 30/70 (mol %) hydrogen/ammonia at 295 K inlet temperature and atmospheric pressure. The stagnation-burner boundary conditions are nominally identical to the experimental data to ensure consistency in strain rate and heat loss. The benefit of the stagnation burner configuration is its steep temperature gradient near the stagnation plate, which allows the Soret effect to be studied for flame quenching regions and provides a temperature boundary condition for comparison to a 1D numerical flame configuration. Furthermore, experimental emissions data enables kinetic validation to improve future kinetic models.

*Corresponding author
E-mail address: kovalevam@cardiff.ac.uk

Numerical simulations were conducted using a detailed reaction mechanism proposed by Gotama et al. [13] which was optimised for laminar burning velocity [13] and found to adequately model emissions of ammonia/hydrogen premixed flames [12]. 1D flame simulations were conducted using Cantera 2.6.0 [14] with the transport properties used to perform the diffusion flux calculations also derived in Cantera. Equations for diffusion velocity and diffusion flux are described in literature [15, 16], where diffusion velocity of species and mass diffusion flux are linked through the species conservation equation, as given by (1):

$$\frac{\partial(\rho y_i)}{\partial t} + \nabla \cdot (\rho \vec{v} y_i) = -\nabla \cdot \vec{j}_i + M_i \dot{\omega}_i \quad (1)$$

Where $\vec{j}_i$ is mass diffusion flux of species i, t is time, ρ is density, M_i is molar weight of species i, $\dot{\omega}_i$ is the reaction rate/source term, $\vec{v}$ is the absolute velocity of species i, y_i is the mass fraction of species i. The mass diffusion flux, j_i can be described as the diffusion component of molecules due to concentration gradient, not only from concentration gradient of species i itself, $\vec{j}_i^d$ but also pressure, $\vec{j}_i^p$ and temperature, $\vec{j}_i^T$ contributions (2):

$$\vec{j}_i = \vec{j}_i^d + \vec{j}_i^T + \vec{j}_i^p \quad (2)$$

Due to low Mach number, the baro-diffusion term, $j_{p,i}$ was considered negligible in this study [8]. The ordinary diffusion term, $\vec{j}_i^d$ was described using either the multi-component (3) or mixture-averaged (4) formulation, in which diffusive flux depends on the concentration gradient of every species or only species i, respectively:

$$\vec{j}_i^d = \frac{\rho M_i}{M_{mixt}} \sum_{j=1,\, j\neq i}^{N} D_{i,j}^{MC} \rho \nabla y_i \quad (3)$$

Where M_{mixt} is the mixture molecular weight, $D_{i,j}^{MC}$ is the multi-component diffusion coefficient, and mass fraction of species i is given as y_i. The mixture-averaged formulation is given by (4), where D_i^M is the mixture-averaged diffusion coefficient:

$$\vec{j}_i^d = D_i^M \rho \nabla y_i \quad (4)$$

Finally, the Soret diffusion flux term, $\vec{j}_i^T$ was calculated using (5):

$$\vec{j}_i^T = -D_i^T \nabla (\ln T) \quad (5)$$

Where the corresponding thermal diffusion coefficient is given as D_i^T for a temperature, T. Finally, in analysing the effect of diffusion modelling, I_R, the integral rate of production (ROP) of species i with respect to reaction R was calculated using (6):

$$I_R = \int_{L1}^{L2} \dot{\omega}_{R,i} dx \quad (6)$$

The lengths used in calculating the integral ROP are as follows: $L1 \approx 0.0115$m and $L2 \approx 0.016$m for lean conditions ($\phi = 0.59$) and $L1 \approx 0.011$m and $L2 \approx 0.015$m for rich conditions ($\phi = 1.2$). These are the locations of the flame zone in the lean region and post-flame zone in the rich region for a flame domain of 0.2m and the rationale for selecting these regions justified in Section 3.

Two conditions for equivalence ratio, ϕ were selected for further analysis in Section 3: one lean, ($\phi = 0.59$) and one rich ($\phi = 1.2$) condition. For lean conditions, an equivalence ratio of 0.59 was chosen to ensure the N_2O concentration reached a sufficiently high value to facilitate analysis. Furthermore, this condition can be representative of ultra-lean combustion systems. A flame with rich equivalence ratio of 1.2 was selected as a point of interest owing to the anticipated levels of NO and H_2 affording potential differences for cases with/without the Soret effect to be observed. Furthermore, this condition corresponds with simultaneously low NO and NH_3 emissions, as reported by Hayakawa et al. [11].

3 Results and Discussion

3.1 The Effect of molecular diffusion modelling on emissions

Figure 1 compares measurements and modelling of the burner-stabilised stagnation flame configuration using various MDM. The comparison shows that the mixture-averaged and multi-component models (without Soret effect) resulted in almost identical predictions. However, the addition of the Soret effect into the multi-component model reduced H_2 and N_2O emissions while simultaneously increasing NO and NO_2 emissions. This suggests that the Soret effect has a significant role in determining the witnessed emissions, requiring the extended chemistry analysis detailed in the sections below.

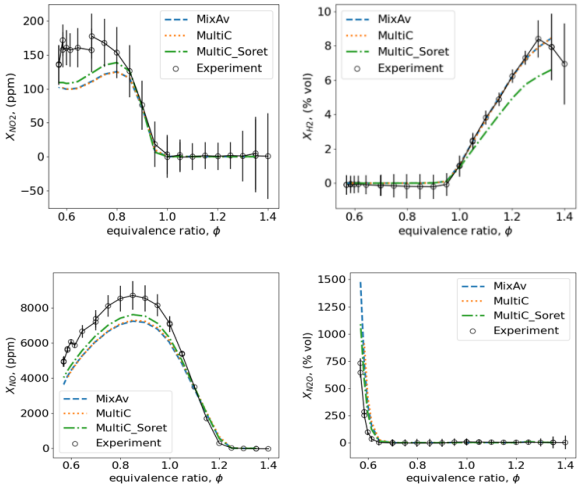

Figure 1: Outlet gas emissions in burner-stabilised stagnation flame with various MDM models and experimental data from Hayakawa et. al [12]

3.2 Analysis of the Soret effect at lean conditions

Figure 2 shows the flame structure at $\phi = 0.59$, demonstrating that when the Soret effect is included, H_2 consumption occurs closer to the burner inlet. As a result, the flame front shifts upstream, extending the high temperature region. This extension encourages fuel decomposition involving high-temperature kinetics, increasing the level of O, H, OH, NH_2, and NH radicals in the flame zone. This drives an increase in NO production in the reaction zone. As the flame zone shifts, N_2O is produced and consumed faster. Despite low O, H, OH radical concentration at the wall, there is also an increase in NO_2 and NO production in this region driven by the Soret effect.

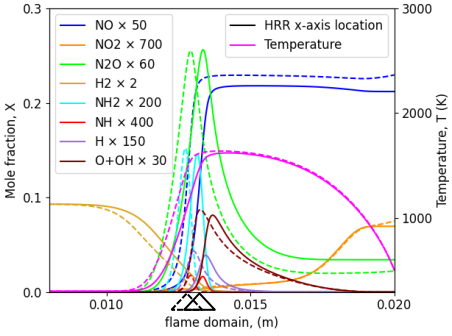

Figure 2: Species and flame structure across the domain at $\phi = 0.59$ (dashed line includes the Soret effect).

To understand the change in species concentrations in Fig. 2, Fig. 3 compares the contribution of diffusion flux from ordinary and Soret (thermal) diffusion of H_2, NO, NO_2, and N_2O species. In this study, a positive diffusion flux means diffusion towards the downstream direction and *vice versa*. Due to the strong temperature change, H_2 experiences a strong positive thermal flux near the flame front. This results in accelerated diffusion of H_2 towards the flame front and accordingly encourages H_2 consumption, leading to a decreased H_2 mole fraction and a shift in the flame front towards the inlet. Another notable trend is also observed for NO_2, where a strong positive thermal flux occurs near the wall, which can be attributed to the steep, negative wall temperature gradient. NO_2 experiences Soret diffusion in the reverse direction, owing to relatively heavier molecules diffusing towards lower temperature regions. Hence, the difference NO_2 emissions seen in Fig. 2 can be directly attributed to Soret diffusion. Meanwhile, the Soret contribution to the diffusion of NO and N_2O molecules is minor.

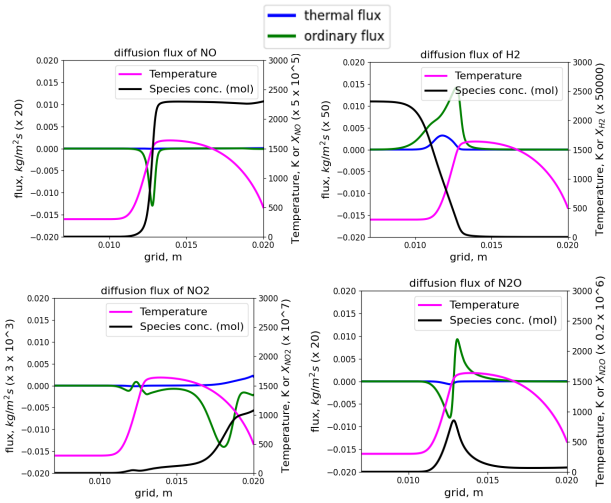

Figure 3: Diffusion flux across domain at $\phi = 0.59$. A positive diffusion flux means diffusion towards the downstream direction and *vice versa*.

To analyse the behaviour of NO and N_2O, ROP graphs for these species are presented in Fig. 4. The total ROP shown in the figure includes all reactions (not only top reactions).

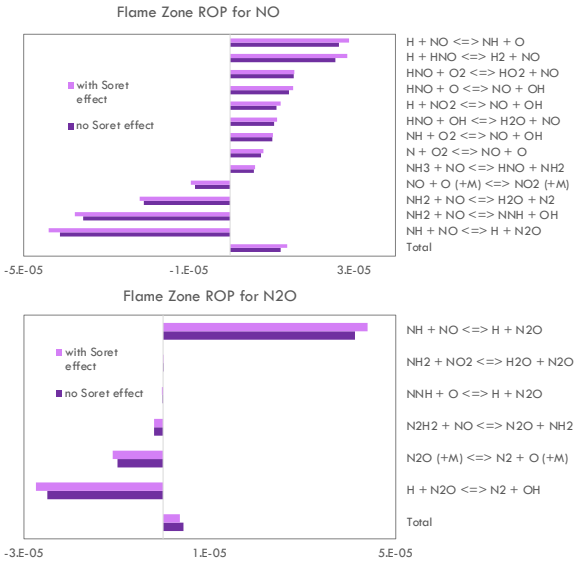

Figure 4: ROP in flame zone for $\phi = 0.59$ (The total value includes all reactions).

As previously discussed, the inclusion of Soret effect leads to an increased pool of O, H, OH, NH_2, and NH radicals (see Fig. 2). Accordingly, this increases the ROP of NO and N_2O, as evident from key NO production reactions, which involve these radicals. For instance, additional H and NH_x radicals promote production and consumption of NO, respectively with the total contribution being an increase in the production of NO. For N_2O, a higher NH radical peak promotes N_2O formation via NH + NO ⇔ H + N_2O, while additional H radical promotes reduction via H + N_2O ⇔ N_2 + OH, with the net effect being a reduction in ROP of N_2O.

3.3 Analysis of the Soret effect at rich conditions

Fig. 5 shows the flame structure at the $\phi = 1.2$ condition.

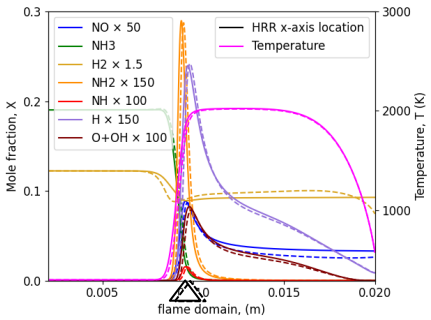

Figure 5: Scaled species and flame structure across domain at $\phi = 1.2$ (dashed line includes the Soret effect).

Similar to the lean case, this figure shows a faster reduction of H_2 in the flame domain due to the Soret effect, but because of the excess fuel, not all H_2 is consumed in the flame zone consequently resulting in a less steep H_2 concentration gradient compared to the lean condition. This resulted in smaller downstream flame shift, with peak concentrations of O, OH, H, NO, NO_2, N_2O, being similar regardless of whether the Soret effect was included. When considering the Soret effect, the rate of NO consumption increases in the post-flame zone and the H_2 profile is affected in both the post-flame zone and at the wall. To understand the direct contribution of the Soret effect to diffusion of species, Figure 6 shows the diffusion flux data for H_2, H, NH_3 and NO.

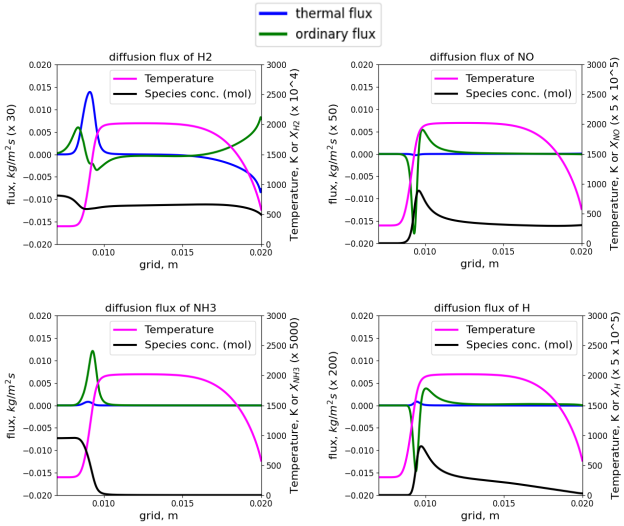

Figure 6: Diffusion flux contribution across domain at $\phi = 1.2$. A positive diffusion flux means diffusion towards the downstream direction and *vice versa*.

Figure 6 suggests that the impact of thermal flux on H_2 is even more significant compared to the ordinary flux at the rich condition. Both H_2 and to a lesser extent, NH_3 are accelerated towards the flame zone by the Soret effect, as shown by positive thermal diffusion flux in this region of the graph. Additionally, near the stagnation wall, a negative thermal flux for H_2 is observed, which encourages H_2 to move upstream, resulting in a higher concentration of H_2 and NH_3 in the region between the flame front and the outlet, as seen in Fig. 5. The large negative thermal flux near the quenching wall suggests that the reduced H_2 concentration in the outlet is directly caused by the Soret diffusion effect at the stagnation wall. By contrast, NO has a negligible thermal diffusion force acting directly on the molecule, indicating that the difference in NO is due to the indirect contribution of Soret diffusion.

To understand the reason behind the lower NO mole fraction, the ROP of NO in the post-flame zone is given in Fig. 7. It shows that the inclusion of Soret effect enhances both NO production and consumption, with a net effect of reducing NO emissions. The promotion in NO production/reduction can be attributed to the enrichment of NH_3 and H_2 in the post-flame zone. This allows more fuel decomposition in this region through reactions with O, H, OH radicals. This in turn results in additional H and NH_x available for NO formation and reduction, respectively.

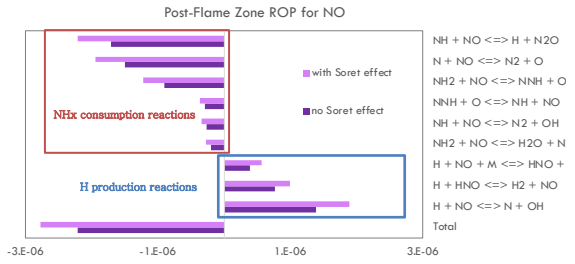

Figure 7: ROP in flame zone for $\phi = 1.2$ (The total value includes all reactions).

4 Conclusions

The impact of the Soret effect on the chemistry of premixed laminar ammonia/hydrogen flames was analysed with the following conclusions:

- Multi-component and mixture-averaged models exhibited similar performance for predicting gaseous emissions of key species (NO, N_2O, NO_2, and H_2).
- The inclusion of Soret effect at lean conditions resulted in a decrease in N_2O emissions and increase in NO and NO_2 emissions. For rich conditions, this effect decreased H_2 and NO emissions. Diffusion flux analysis shows that the reduction of H_2 and increase in NO_2 are attributed to Soret diffusion acting directly on these molecules. Conversely, the reduction of N_2O and change in NO are indirectly caused by Soret diffusion affecting the flame chemistry.
- In the lean case, the temperature profile shifts upstream. In the rich case, the temperature profile shifts only slightly downstream.
- In both lean and rich conditions, the Soret effect accelerates the diffusion of H_2 towards the flame front. In the lean case, this causes faster consumption of H_2 and accelerates high temperature kinetics for higher production of O, H, OH, NH_2, and NH radicals in the flame zone, increasing the rate of NO production. At rich conditions, higher levels of NH_3 and H_2 lead to more H and NH_x radicals available in the post-flame zone, resulting in net-NO reduction.

5 Acknowledgment

Part of this study was supported by the collaborative research project of the Institute of Fluid Science, Tohoku University (project code: J22I086).

References

[1] J. Otomo, M. Koshi, T. Mitsumori, H. Iwasaki, K. Yamada, Int. J. Hydrogen Energy 43 (2018) 3004–3014.

[2] N.J. Brown, L.A.J. Bastien, P.N. Price, Prog. Energy. Combust. Sci. 37 (2011) 565–582.

[3] C.K. Law, Combustion Physics, Cambridge University Press, 2010.

[4] A.J. Fillo, J. Schlup, G. Blanquart, K.E. Niemeyer, Combust. Flame 223 (2021) 216–229.

[5] C. Chi, W. Han, D. Thévenin, Proc. Combust. Inst. (In-Press) (2022).

[6] M. Faghih, W. Han, Z. Chen, Combust. Flame 194 (2018) 175–179.

[7] J. Liu, X. Zhang, T. Wang, X. Hou, J. Zhang, S. Zheng, Int. J. Hydrogen Energy 40 (2015) 8475–8483.

[8] J.F. Grcar, J.B. Bell, M.S. Day, Proc. Combust. Inst. 32 (2009) 1173–1180.

[9] C. Netzer, A. Ahmed, A. Gruber, T. Løvås, Combust. Flame 232 (2021) 111520.

[10] Z. Zhou, F.E. Hernández-Pérez, Y. Shoshin, J.A. van Oijen, L.P.H. de Goey, Combust. Theory and Modelling 21 (2017) 879–896.

[11] D. Wang, C. Ji, S. Wang, J. Yang, Z. Wang, Int. J. Hydrogen Energy 46 (2021) 2667–2683.

[12] A. Hayakawa, H. Masao, M. Kovaleva, G.J. Gotama, E.C. Okafor, S. Colson, S. Mashruk, A. Valera-Medina, T. Kudo, H. Kobayashi, Proc. Combust. Inst. (In-Press) (2022).

[13] G.J. Gotama, A. Hayakawa, E.C. Okafor, R. Kanoshima, M. Hayashi, T. Kudo, H. Kobayashi, Combust. Flame 236 (2022) 111753.

[14] D.G. Goodwin, R.L. Speth, H. Moffat, B. Weber, Cantera: An Object-oriented Software Toolkit for Chemical Kinetics, Thermodynamics, and Transport Processes, (2021).

[15] K.K. and R. Acharya, Laminar Premixed Flames, in: Fundamentals of Turbulent Multiphase Combustion, 2012: pp. 43–124.

[16] E. Stanley, Tech. Lisboa. (2018). Available at: https://slideplayer.com/slide/13268883/